ORIGINAL ARTICLE

Molecular Characterization and Potential Inhibitors Prediction of Protein Arginine Methyltransferase-2 in Carcinoma: An Insight from Molecular Docking, ADMET Profiling and Molecular Dynamics Simulation Studies

Md Sahadot Hossen[1], Md Nur Islam[2], Md Enayet A Pramanik[3], Md Hasanur Rahman[4], Md Al Amin[5], Saraban T Antora[6], Farzana S Sraboni[7], Rifah N Chowdhury[8], Nazia Farha[9], Amina A Sathi[10], Samia Sadaf[11], Farjana Banna[12], Md Rezaul Karim[13], Nasrin Akter[14], Md Royhan Gofur[15], Md Shariful Islam[16], M Morsed Z Miah[17], Mira Akhter[18], Md Shariful Islam[19], Md Sharif Hasan[20], Fahmida Fahmin[21], Mohammad M Rahman[22], Prabir M Basak[23], Amio K Sonnyashi[24], Haimanti S Das[25], Mamun Al Mahtab[26], Sheikh MF Akbar[27]

Received on: 12 June 2024; *Accepted on*: 13 August 2024; *Published on*: 27 December 2024

Abstract

Objectives: To predict and characterize the three-dimensional (3D) structure of protein arginine methyltransferase 2 (PRMT2) using homology modeling, besides, the identification of potent inhibitors for enhanced comprehension of the biological function of this protein arginine methyltransferase (PRMT) family protein in carcinogenesis.

Materials and methods: An *in silico* method was employed to predict and characterize the three-dimensional structure. The bulk of PRMTs in the PDB shares just a structurally conserved catalytic core domain. Consequently, it was determined that ligand compounds may be the source of co-crystallized complexes containing additional PRMTs. Possible PRMT2 inhibitor compounds are found by using S-adenosyl methionine (SAM), a methyl group donor, as a positive control.

Results: Protein arginine methyltransferases are associated with a range of physiological processes, including as splicing, proliferation, regulation of the cell cycle, differentiation, and signaling of DNA damage. These functional capacities are also related to carcinogenesis and metastasis-several forms of PRMT have been cited in the literature. These include PRMT-1, PRMT-2, and PRMT-5. Among these, the role of PRMT-2 has been shown in breast cancer and hepatocellular carcinoma. To gain more insights into the role of PRMT2 in cancer pathogenesis, we opted to characterize tertiary structure utilizing an *in silico* approach. The majority of PRMTs in the PDB have a structurally conserved catalytic core domain. Thus, ligand compounds were identified as a possible source of co-crystallized complexes of other PRMTs. The SAM, a methyl group donor, is used as a positive control in order to identify potential inhibitor compounds of PRMT2 by the virtual screening method. We hypothesized that an inhibitor for other PRMTs could alter PRMT2 activities. Out of 45 inhibitor compounds, we ultimately identified three potential inhibitor compounds based on the results of the pharmacokinetics and binding affinity studies. These compounds are identified as 3BQ (PubChem CID: 77620540), 6DX (PubChem CID: 124222721), and TDU (PubChem CID: 53346504). Their binding affinities are −8.5 kcal/mol, −8.1 kcal/mol, and −8.8 kcal/mol, respectively. These compounds will be further investigated to determine the binding stability and compactness using molecular dynamics simulations on a 100 ns time scale. *In vitro* and *in vivo* studies may be conducted with these three compounds, and we think that focusing on them might lead to the creation of a PRMT2 inhibitor.

Conclusion: Three strong inhibitory compounds that were non-carcinogenic also have drug-like properties. By using desirable parameters in root mean square deviation (RMSD), root mean square fluctuation (RMSF), radius of gyration (Rg), solvent accessible surface area (SASA), molecular surface area (MolSA), and intermolecular hydrogen bonding, complexes verified structural stability and compactness over the 100 ns time frame.

Keywords: Computer-aided drug design, Homology modeling, Inhibitor's prediction, Molecular docking, Molecular dynamics simulation, Protein arginine methyltransferase 2.

Euroasian Journal of Hepato-Gastroenterology (2024): 10.5005/jp-journals-10018-1443

Introduction

Protein arginine methyltransferases (PRMTs), or protein arginine N-methyltransferases, are a specific group of enzymes found in eukaryotes. They are responsible for transferring methyl groups from the co-substrate S-adenosyl-L-methionine (SAM or Ado-Met) to the guanidine nitrogen atoms in arginine residues of target proteins. This process leads to the creation of methyl arginine and S-adenosyl homocysteine (SAH or Ado-Hcy) as the final product and a side product, respectively.[1] The PRMT-mediated arginine methylation has received most attention for

[1]Department of Biochemistry and Molecular Biology, School of Life Sciences, Shahjalal University of Science and Technology, Sylhet, Bangladesh

[2]National Laboratory of Biomacromolecules, Chinese Academy of Sciences Center for Excellence in Biomacromolecules, Institute of Biophysics, CAS, Beijing, People's Republic of China; Department of Pharmacy, Manarat International University, Gulshan, Dhaka, Bangladesh

[3]Department of Entomology, On-Farm Research Division, Bangladesh Agricultural Research Institute, Terokhadia, Rajshahi, Bangladesh

its crucial cellular regulations including cell growth, transcription regulations, RNA splicing and transport, signal transduction, DNA repair, differentiation and embryogenesis, and nuclear/cytoplasmic shuttling.[2–10] It's becoming clear that in epigenetics and oncology, PRMT family proteins are involved in maintaining normal physiologic processed as well as disease pathogenesis. Three major types of methyl arginine are known to generate: dimethylarginine (SDMS), each of which has potentially different functional consequences.[8,10,11] Up to date, nine members of PRMT family have been identified in higher eukaryotes namely PRMT1 to PRMT9. These nine PRMTs members further classified into three types: (PRMT-1, 2, 3, 4, 6 and 8) belongs to type I PRMTs and convert arginine to ADMA, (PRMT5 and PRMT9) belongs to type II PRMTs which generate MMA.[1,12–14] Despite the identification of several hundred crystal structures of several PRMTs, a shortage of structural data and limited methyl transferase activity have prevented the characterization of the crystal structure of PRMT2 at the structural level.

Protein arginine methyltransferase 2 is implicated in numerous biological functions and plays a pivotal role in governing key cellular processes. The PRMT2 functions as a transcriptional co-activator in a manner that depends on the presence of a ligand. It interacts with nuclear receptors such as estrogen receptor alpha, retinoic acid receptor, and androgen receptor, and boosts the transcriptional activity of these hormone receptors.[15,16] Recent studies have demonstrated the role of PRMT2 in the development of cancer and the spread of cancer cells, particularly in breast cancer.[17] In addition to its role as an important biological marker, PRMT2 negatively regulated the expression of CCND1 in breast cancer cells, regulation the defective expression level of CCND1. It is widely recognized that the control of Cyclin D1 (CCD1) plays a crucial role in both cell proliferation and tumor growth. The overexpression of CCD1 in breast cancer cells proliferation is caused by the down regulation of PRMT2, which activates the Akt/GSK-3b/CCND1 signaling pathway.[18–20] Furthermore, PRMT2 governs the activity of E2F by interacting with the retinoblastoma gene family (RB). The PRMT2 and E2F work together to control the course of the cell cycle.[18] In addition, potential role in the regulation of leptin-STAT3 melanocortin pathway in the treatment of obesity and obesity-related syndromes and interaction with 1B associated protein (E1B-AP5) also describes.[21,22]

The PRMT2 was initially discovered through its sequence similarity to the human PRMT1 gene and the genome of yeast methyltransferase HMT1 gene.[23] It contains an Ado-met/SAM-binding domain and N-terminal Src homology 3 (SH3) domain that recognizes proline-rich protein motifs.[23,24] The two domains are linked by cis-proline protein motifs that are conserved with strictness.[23] Both of the domains are linked by a cis-proline 254 that is preserved with high precision. The PRMT2 methylates histone H4 and like PRMT1, it can methylate a fusion protein of glutathione transferase (GST) and the glycine–arginine region/patches (GAR motifs) of human fibrillarin.[23] However, further study needs to be carried out about the structural and enzymatic activity of PRMT2.

Recently, the crystal structure of the PRMT2 catalytic module from zebrafish (*Danio rerio*) and from mouse (*Mus musculus*) has been described.[25] In mammals, however, no significant study has yet been reported about the three-dimensional structure of PRMT2. The objective of this work is to use homology modeling to predict and describe the three-dimensional structure of PRMT2. Additionally, the study aims to identify strong inhibitors in order to

[4]Department of Biotechnology and Genetic Engineering, Faculty of Life Sciences, Bangabandhu Sheikh Mujibur Rahman Science and Technology University, Gopalganj, Bangladesh

[5]Department of Biotechnology and Genetic Engineering, Faculty of Life Sciences, Mawlana Bhashani Science and Technology University, Tangail, Santosh, Bangladesh

[6]Department of Biochemistry and Molecular Biology, Faculty of Life Sciences, Bangabandhu Sheikh Mujibur Rahman Science and Technology University, Gopalganj, Bangladesh

[7,10]Department of Genetic Engineering and Biotechnology, Faculty of Biological Sciences, University of Rajshahi, Rajshahi, Bangladesh

[8]Department of Pharmacy, Faculty of Pharmacy, University of Dhaka (DU), Mokarram Hussain Khundker Bhaban, University St, Dhaka, Bangladesh

[9]Department of Genetic Engineering and Biotechnology, Faculty of Biological Sciences, University of Chittagong, Chittagong, Bangladesh

[11]Department of Biology, Development Biology Laboratory, Clarkson University, Potsdam, New York, United States of America

[12]Department of Biotechnology and Genetic Engineering, Faculty of Science, Islamic University, Kushtia, Bangladesh

[13]Department of Pharmacy, School of Engineering, Science and Technology, Manarat International University, Gulshan, Dhaka, Bangladesh

[14]Department of Biochemistry and Molecular Biology, University of Rajshahi, Rajshahi, Bangladesh

[15,16]Department of Veterinary and Animal Sciences, University of Rajshahi, Rajshahi, Bangladesh

[17]Department of Hematology, Rajshahi Medical College, Rajshahi, Bangladesh

[18]Department of Clinical Pathology, Rajshahi Medical College Hospital, Rajshahi, Bangladesh

[19]Department of Ortho-Surgery, Rajshahi Medical College, Rajshahi, Bangladesh

[20]Department of Cardiology, Mymensingh Medical College Hospital, Mymensingh, Bangladesh

[21]Department of Paediatric, Mymensingh Medical College Hospital, Mymensingh, Bangladesh

[22–24]Department of Medicine, Rajshahi Medical College, Rajshahi, Bangladesh

[25]Department of Virology, Rajshahi Medical College, Rajshahi, Bangladesh

[26]Department of Interventional Hepatology, Bangabandhu Sheikh Mujib Medical University, Shahbagh, Dhaka, Bangladesh

[27]Department of Gastroenterology and Metabology, Ehime University Graduate School of Medicine, Ehime, Japan

Corresponding Author: Md Enayet A Pramanik, On-Farm Research Division, Bangladesh Agricultural Research Institute, Terokhadia, Rajshahi, Bangladesh, Phone: +880 1744530588; +880 1718614674, e-mail: enayet.bari.bd@gmail.com

How to cite this article: Hossen MS, Islam MN, Pramanik MEA *et al*. Molecular Characterization and Potential Inhibitors Prediction of Protein Arginine Methyltransferase-2 (PRMT2) in Carcinoma: An Insight from Molecular Docking, ADMET Profiling and Molecular Dynamics Simulation Studies. Euroasian J Hepato-Gastroenterol 2024;14(2): 160–171.

Source of support: Nil

Conflict of interest: Dr Mamun Al Mahtab and Dr Sheikh MF Akbar are associated as the Editorial board members of this journal and this manuscript was subjected to this journal's standard review procedures, with this peer review handled independently of these Editorial board members and their research group.

gain a deeper knowledge of the biological function of this protein from the PRMT family.

Materials and Methods

Protein Sequence Retrieval and Prediction of Secondary Structure

The amino acid sequence of human PRMT2 was acquired in FASTA format from the UniProt Knowledgebase (UniProtKB) database (https://www.uniprot.org), which serves as a repository for meticulously curated protein data with comprehensive, precise, and consistent annotation.[26] The protein is identified by its primary accession number, P55345, and consists of 433 amino acids. The ProtParam server was used to determine the physiochemical characteristics (https://web.expasy.org/protparam/). The PSIPRED and SOPMA tools were used to estimate the secondary structure.[27,28] The protein's secondary structure consists of various elements, including α helix, 310 helix, pi helix, beta bridge, prolonged strand, beta turns, bend area, random coil, ambiguous states, and others. The SOPMA employs homologous protein identification, sequence alignment, and a conformational score determination method to forecast these characteristics. The correlation co-efficient value confirmed the precision of the forecast. The amino acid sequences were inputted in a plain text format, and the default parameters were specified.

Tertiary Structure Prediction and Refinement

The 3D structure of human PRMT2 was modeled based on the available crystal structure template deposited in the Protein Data Bank (PDB). The template was selected from the template identification wizard of Swiss Model. Few parameters were considered while selecting template and they are global structure quality estimation (GMQE), quaternary structure quality estimation (QSQE), and sequence identity, methods of the template structure determination and the resolution of the structure.[29] To obtain a stable conformation of the predicted protein, YASARA online energy minimization server was utilized.[30] For the visualization purpose, BIOVIA discovery studio was used.[31]

Model Evaluation and Validation

The stereo chemical quality of the protein 3D structure and its overall structural geometry were confirmed using PROCHECK, ERRAT and VERIFY3D.[32,33] The Ramachandran plot statistics were examined in order to assesses the stability of the model and the validation of the residues.[34] Additionally, root mean square deviation (RMSD) was used by the superposition of the query and the template structure via PyMOL to measure the quality of the model.[35]

Molecular Docking Analysis

Ligand Retrieval and Preparation

Phytochemical information based on their inhibitory activity total 45 ligands were retrieved though literature search.[36,37] The 3D structure of phytochemicals were saved in SDF format from the PubChem database and permuted into PDB files by using PyMOL.[38,39] Phytochemical's energy minimization was done by using Avogadro tools.[40,41]

Active Site Prediction

The active site of the modeled protein was predicted by the web server CASTp (http://surl.li/cgnks). The default probe radius of 1.4 Å was used, and the area, volume, and sequence ID were calculated.[42]

Structure-based Virtual Screening and Molecular Docking

To get started, PyRx, PyMOL, and BIOVINA discovery studio were utilized for structure-based virtual screening bioinformatics tools. The RCSB PDB and PubChem database are excellent sources for protein data retrieval, assessment, and analysis.

The mechanism of interactions and binding of phytochemicals with the homology model of PRMT2 was determined by molecular docking approach. The small molecules that were obtained and the expected PRMT2 were submitted into the PyRx virtual screening tool. The target protein completed conversion into macromolecules, while phytochemicals were transformed into ligands. Additionally, atomic coordination was modified into PDBQT format. The parameters and grid box are set to a standard value, with the center box positioned at $X = -14.5754$, $Y = -1.6991$, $Z = 18.9045$. The dimensions of the box are $X = 46.9649990368$, $Y = 73.9918595886$, $Z = 67.7502706909$ Å. Subsequently, the docking data performed screening to determine their binding affinity, and all feasible docked conformations were then saved in CSV format. Only the conformations that exclusively interacted with the active-site residues of the targeted PRMT2 protein were examined. Detailed interactions were then investigated using Discovery Studio and PyMOL. The docking results were given as a negative score in kcal/mol, with the lowest value representing the maximum binding affinity.

Ligand-based ADME and Toxicity Prediction

The pharmacokinetic characteristics of extremely small molecules were assessed using the online program Swiss ADME. Lipinski's rule of five indicates that a molecule is likely to have desirable drug-like qualities if it meets at least four out of five criteria. These criteria include having a molecular weight of 500 Daltons, hydrogen bond acceptor ≤5, hydrogen bond donor ≤10, lipophilicity <5, and a molar refractivity value between 40 and 130. Compounds that satisfy Lipinski's criteria are considered to be optimal prospects for medication development. The admetSAR tool was utilized to forecast the toxicological characteristics of specific chemicals. The prediction included AMES toxicity, carcinogenicity, hepatoxicity, oral acute rat toxicity (LD50), and suppression of hERG I and II.

Molecular Dynamics Simulation

The "Desmond v3.6 Program" in Schrödinger (https://www.schrodinger.com/) was used to conduct a molecular dynamic simulation of the suitable three complexes; PRMT2-CID:124222721, PRMT2-CID:53346504, and PRMT2–CID:77620540. The OPLS3e force field is one of the variants of the optimized potential for ligand simulations (OPLS) force field that was used to compute the potential energy of the complexes inside the solvency system; it is suggested that it has higher accuracy in the protein–ligand binding.[43] The default TIP3P water model was utilized to build the solvent within the orthorhombic periodic boundary condition at 10 Å distances. A value of 0.15 M salt has randomly distributed inside the solvent system. Using NPT ensembles, the equilibrium procedure was conducted out for 50 ps at 1.2 kcal/mol, with the Nose–Hoover and isotropic methods held at 300 K and one atmosphere pressure.

The protein–ligand complex's sustainability was assessed using the RMSD, root-mean-square fluctuation (RMSF), radius of gyration (Rg), solvent accessible surface area (SASA), molecular surface area (MolSA), and intermolecular interactions fraction.

Results and Discussion

Secondary Structure Prediction and Physiochemical Properties

The ProtParam and SOMPA analyzed the physiochemical properties and secondary structure. The ProtParam server calculated analogous properties of PRMT2's building blocks, and the number of amino acids reported is 30530, molecular weight is 32532510.61 kDa, and theoretical isoelectric point (PI) is 4.34. The PI values suggest protein is acidic. There are no adversely (Asp + Glu) and definitely (Arg + Cys) charged buildups, thus the desired protein is charge neutral and constitutes 25.9% Ala (A), 24.5% (G), and 28.6% Thr (T) amino acid residues.

Using secondary structure analysis to predict protein function and structure is becoming more common. Secondary structure parameters of PRMT2 in human contain alpha helix, extended strand, and random coil with a percentage of 26.33, 24.02, and 49.65, respectively (Table 1).

Table 1: Percentages of secondary structure components of PRMT2 in human by SOMPA

Secondary structure	*Number of residues*	*Percentage (%)*
Helix (Hh)	114	26.33
Helix (Gg)	0	0.00
pI helix (Ii)	0	0.00
Beta bridge	0	0.00
Extended strand	104	24.02
Beta turn	0	0.00
Bend region	0	0.00
Random coil	215	49.65
Ambiguous state	0	0.00
Other states	0	0.00

Tertiary Structure and Quality of Modeled Protein

The three-dimensional structure of the focused PRMT2 was displayed in Swiss-model via selection of the one top suitable template (5ful.1), and the target arrangement was based on the result of qualitative model energy analysis (QMEAN) score of 0.67, global model quality estimate (GMQE) score of 0.74, sequence identity 88.18%, and the method by which the structure was determined. The less the resolution of the crystal structure is available, the better the quality. Therefore, the X-ray crystallographic structure with 1.9 is the best structure available and was selected as a template. A total of 40 templates were found and the top 5 of them are arranged in the Table 2.

The template (5ful.1) was used to create the model of a target protein obtain from the RCSB-PDB database. It is the crystal structure of PRMT2 of *Mus musculus*. The template structure is a homodimer protein, containing two polypeptide chains, e.g., A and B chains.

The tertiary structure was predicted and further modified by using the YASARA online energy minimization server for getting the more structurally suitable one. Before energy minimization, the calculated energy was –310625.4 KJ/mol, though after minimization it was –3931136.1 KJ/mol. The superposition of template and model was done by PyMOL and appeared a RMSD after energy minimization esteem of 0.278 and proved efficiently a high level of similarity. The showing superposition of the template and model structure, which were red and blue colored, respectively (Fig. 1).

The PROCHECK evaluated validation of the anticipated structure through Ramachandran plot analysis appeared in Figure 2, where the distribution of angles in the model within the limits and the favored, allowed, and generously allowed zones are symbolized by the red, brown, and yellow color region, respectively.

Parameters like the favored, allowed, and generously allowed regions, as well as the G-factor are key factors for determination of a good model.[44] The 3D structure appraisal was determined by Ramachandran plot appeared that 91.6% of the full buildups were found within the core (A, B, L); in the additional allowed regions (a, b, l. p) 7.8% of residue was found; the generously allowed regions (a, b, l, p) contained 0.3% of residue, as well as 0.3% of residues, were also obtained in the disallowed regions. Among the total residues, non-glycine, and non-proline residues were 604, which was the indication of 100%; the end-residues (excluding Gly and Pro)

Table 2: Template results 5 out of 40 from Swiss-Model template identification wizard

Templates	*Coverage*	*GMQE*	*QSQE*	*Identity*	*Method*	*Oligo state*
1	5ful.1.A Crystal structure *of Mus musculus* PRMT2 with SAH	0.82	0.72	88.19	X-ray 1.9	Homo-dimer
2	5ful.1.A Crystal structure of *Mus musculus* PRMT2 with SAH	0.82	0.72	87.73	X-ray 1.9	Homo-dimer
3	5fub.1.A Crystal structure of zebrafish PRMT2 catalytic domain with SAH	0.72	0.77	59.40	X-ray 2.0	Homo-dimer
4	5fub.1.A Crystal structure of zebrafish PRMT2 catalytic domain with SAH	0.72	0.77	59.82	X-ray 2.0	Homo-dimer
5	5g02.1.A Crystal structure of zebrafish PRMT2 with SFG	0.72	0.47	59.52	X-ray 2.5	Homo-dimer

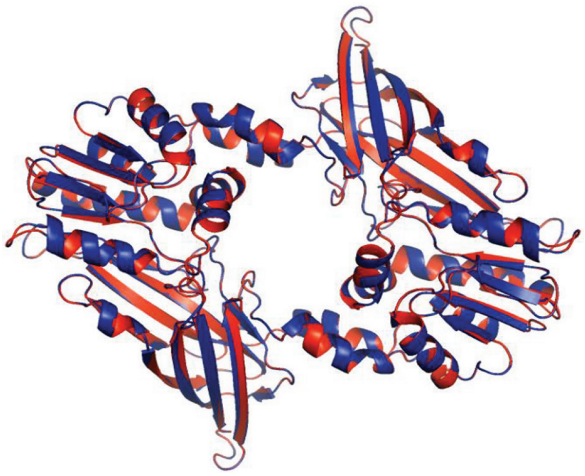

Fig. 1: Superposition presentation of the template and model structure in which the red color demonstrates the template structure and blue color represents the model structure

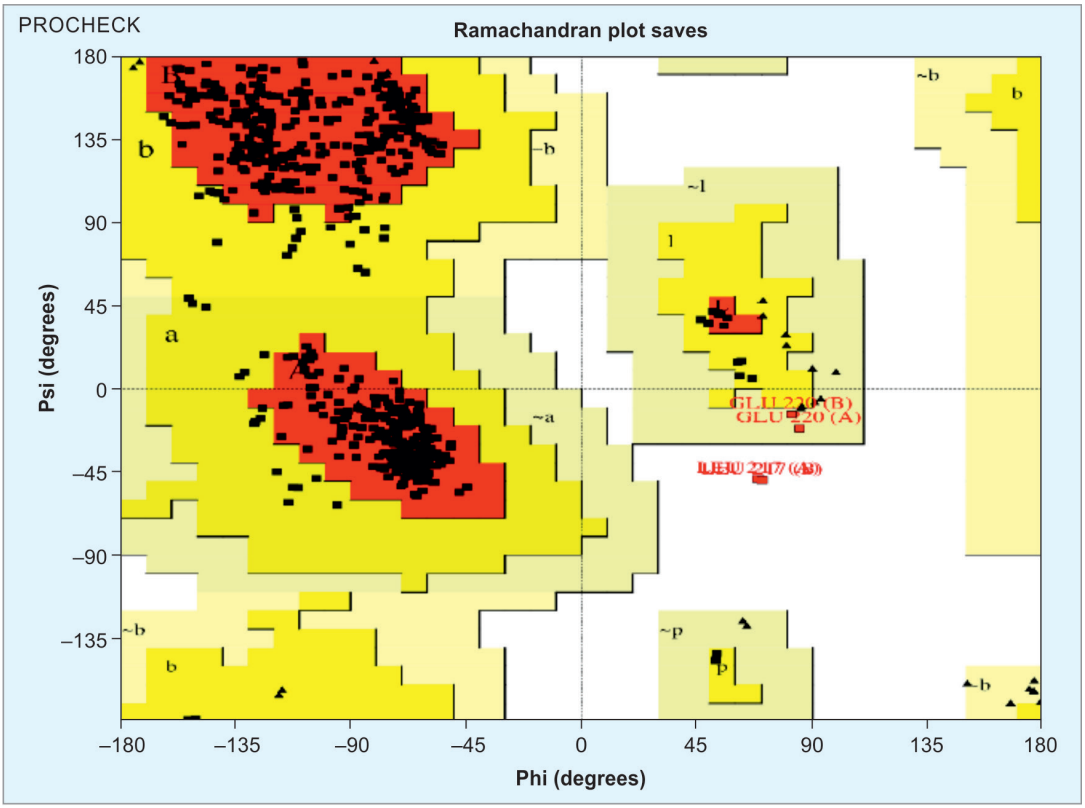

Plot statistics

Residues in most favored regions [A,B,L]	553	91.6%
Residues in additional allowed regions [a.b,l.p]	47	7.8%
Residues in generously allowed regions |~a, ~b, ~l, ~p|	2	0.3%
Residues in disallowed regions	2	0.3%
Number of non-glycine and non-proline residues	604	100.0%
Number of end-residues (excl. Gly and Pro)	6	
Number of glycine residues (shown as triangles)	34	
Number of proline residues	34	
Total number of residues	678	

Based on an analysis of 118 structures of resolution of at least 2.0 Angstroms and R-factor no greater than 20%, a good quality model would be expected to have over 90% in the most favored regions

Fig. 2: Ramachandran plot statistics for modeled PRMT2 protein structure

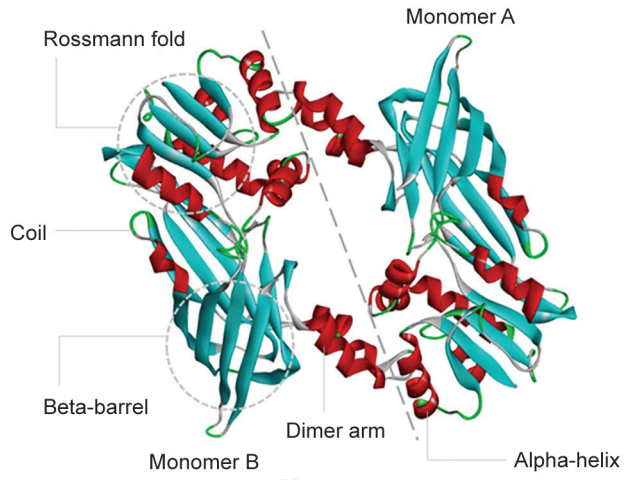

Fig. 3: Three-dimensional representation and domain annotation of modeled PRMT2

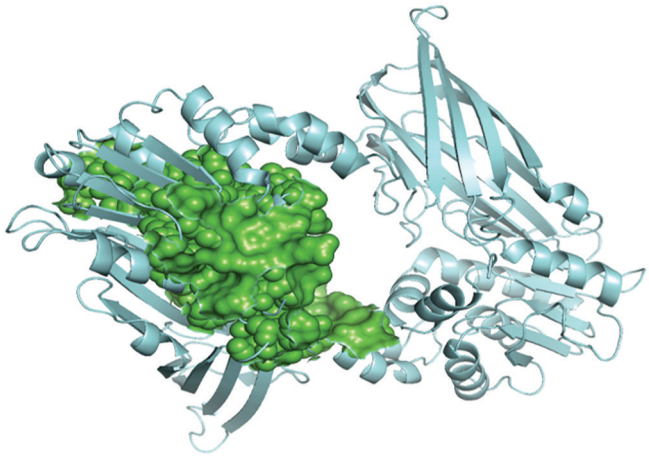

Fig. 4: Representation of predicted active site area (shows as spheres and surface) on a single monomer A of modeled PRMT2

were 4; the glycine residues and proline residues were 34 and 34, accordingly.

However, structure validation and Ramachandran plot analysis, Verify3D, and ERRAT server confirmed the established three-dimensional structure model for the desired target sequence. However, the Verfi3D graph showed that 87.13 of the buildups have an average 3D–1D score of 0.2, which outlines that the natural profile of the model is good. The, by and large, quality factor anticipated using the ERRAT server was 97.572, demonstrating a much better model. The three-dimensional structure of modeled PRMT2 is shown in Figure 3.

Active Site Prediction

An active site is usually a small region compared with the enzyme (10–20% volume of an enzyme) responsible for binding a substrate molecule and undergoing a chemical reaction. The area and volume were determined to be 2853.876 m^2 and 720.473 m^3, respectively. Active site area on a single monomer A of modeled PRMT2 shown in Figure 4. The sequence ID, chain, and amino acid code for the active site are shown in Supplementary Table 1.

Computational Molecular Docking Studies

In computer-aided drug design (CADD), molecular docking is one of the foremost broadly used procedures for discovering novel drugs.[45,46] We selected our hypothesized protein for molecular docking and further MD simulation studies in this experiment. Forty-five small compounds were chosen as ligands with their inhibitory activity against PRMTs through a literature search.[37]

Firstly, molecular docking analysis was carried out, and the retrieved compounds were shown in Supplementary Table 2. The docking score of this study indicates the strength of the chemical-protein binding activity. An initial validation is made using the binding energy of the molecular docking simulation. The compounds with greater binding affinity than SAM (–7.2 kcal/mol) were considered for further analysis. Researchers used SAM as a positive control inhibitor against the PRMT family.[47,48] Furthermore, a re-docking approach was conducted to compare the binding affinity of chosen compounds with their corresponding PDB structure. Surprisingly, all the selected compounds showed greater binding affinity than their corresponding PDB structure.

Therefore, a total of eight ligands were docked with PRMT2 protein, and the binding energy of each ligand is listed in Table 3, where interaction residues of PRMT2 with selected compounds are described. Additionally, among the eight ligands, the representation of binding interaction of protein residues with selected ligands 3BQ, TDU, and 6DX is shown in Figures 5 to 7, respectively. The results of virtual screening binding affinity studies indicate that all compounds bind to active site residues.

Drug-likeness and Toxicological Studies of the Selected Compounds

Monitoring and checking the drug-likeness characteristics as a preliminary screening of drug discovery processes has been used in the recent past. The drug-like properties of the compounds chosen based on their highest binding affinity were later predicted using the online-based Swiss ADME server (Supplementary Table 3). Except for 6DX, 6D3, and 78G, five of the eight compounds adhere to the drug-like properties, acceptable molecular weight range, hydrogen bond acceptor and donor range, and high GI absorption. Toxicological properties calculations suggest that carcinogenic effect are absent for all the compounds and only 3ZG showed AMES toxic, indicating that the threat of mutagenicity is absent for most of the compounds. All of the chosen compounds were invented to be frail hERG I inhibitors. Additionally, weak rat acute toxicity are shown with a median lethal dose (LD50) ranging from 1.743 to 2.713 mol/kg for the selected compounds (Supplementary Table 4).

Molecular Dynamics Simulation

Root Mean Square Deviation Analysis

For the determination of the structural stability of the complex's protein–ligand interaction molecular dynamics simulation study were used. The average change in spatial differences between a docked complex and a post-simulation complex structure is measured using an RMSD analysis. During the 100 ns simulation, the first protein structure (C, backbone, side chain, and heavier atom) was followed by protein-fit ligand aligned and assessed, where the RMSD value was calculated by the equation below:

$$\mathrm{RMSD}_x = \sqrt{\frac{1}{N}\sum_{i=1}^{N} \left(r_i'(t_x) - r_i(t_{ref})\right)^2} \quad \cdots\cdots\cdots 1$$

Table 3: Results of molecular docking analysis of modeled PRMT2 and binding affinity of selected compounds with corresponding PDB

	Ligand identity		*Binding interaction of modeled PRMT2*		*Docking score (kcal/mol)*	
Ligand no.	*PubChem CID*	*Name*	*Hydrogen bond interaction residues*	*Hydrophobic bond interaction residues*	*With Modeled PRMT2*	*With corresponded PDB structure*
3	70678415	KTD	GLU220, ASN291, HIS369	TYR102, TYR290, ARG403	−8.4	−6.8
4	77620540	3BQ	GLU220, ASN291, HIS369, SER105	HIS369, ARG403, TYR102	−8.5	−8.4
5	90642938	3ZG	TYR102, TYR106, GLU220, AS291, TRP370, GLU211	TYR106, HIS369, MET115	−9.2	−7.7
6	53346504	TDU	GLU220, ASN291, HIS369	TYR290, ARG403, TYR102	−8.1	−7.8
11	124220671	6D3	ASN291, SER105, GLU211, MET213, GLU220, GLU114, ASN291, HIS369, TYR106	GLU220, HIS369	−8.1	−7.9
12	124222721	6DX	ARG121, CYS146, GLU211, GLU168, MET213, TRP212, GLY214, GLU220, GLY145		−8.8	−7.6
40	129900308	78G	THR215, LYS371, GLNN98, SER105, GLU114, GLN98, THR215, GLY214, SER105		−8.1	−7.5
44	92205686	A0S	GLU220	LEU111, TRP432, TYR102, HIS404	−8.1	−6.3

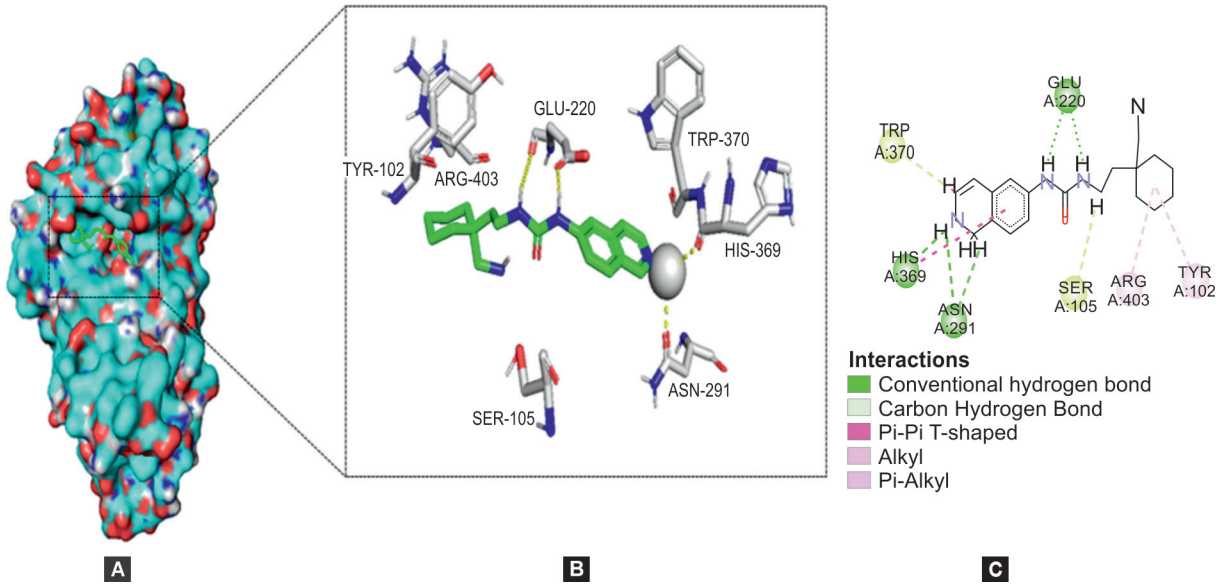

Figs 5A to C: Binding mode and chemical interaction of ligand compound 3BQ with PRMT2, (A) Solid surface structure of PRMT2, where ligand was colored as green, binding on active site; (B) Three-dimensional representation of 3BQ with interacted residues on active site; (C) Two-dimensional representation of binding interaction diagram of 3BQ with PRMT2

Where, N indicates the number of atoms; t_{ref} denotes the reference time; and r is the system x bit chosen after superimposing the reference system's point.

The average change in the area of RMSD of the protein–ligand complex is impeccably satisfactory, with a extend of 1–3 Å, and a more prominent esteem indicates the protein structure has experienced a noteworthy conformational alter. The three complexes, PRMT2-CID: 124222721, PRMT2-CID: 53346504, and PRMT2-CID: 77620540, show an overall low RMSD value (Fig. 8).

The regular and consistent RMSD average (1.7 Å) during 100 ns simulation, which strongly coincides with docking results, indicates the ligand's robust binding to the protein.

Root Mean Square Fluctuation Analysis

Root mean square fluctuation is a calculation of individual residue flexibility which measures the average displacement of residues over time from a fixed position and is typically plotted vs

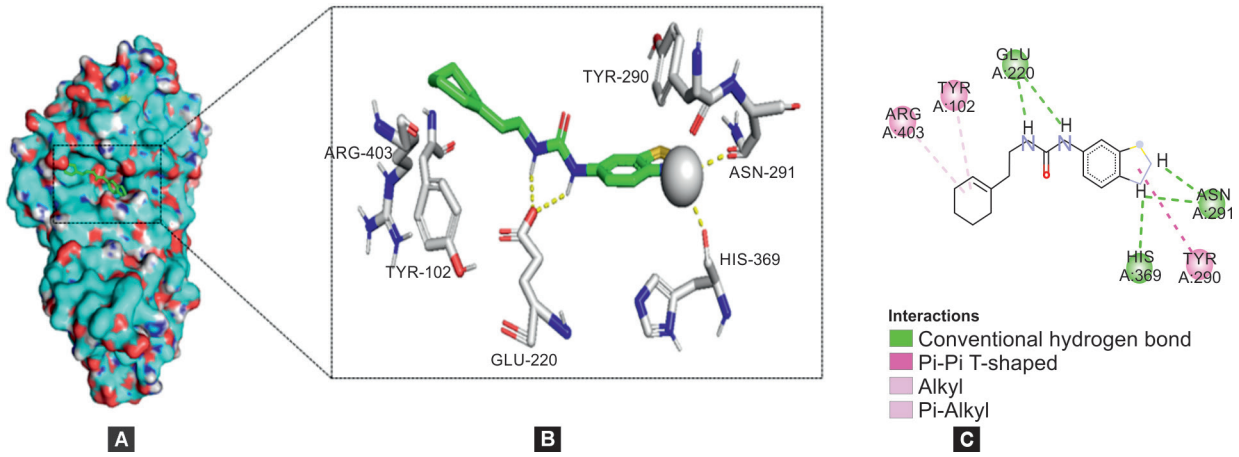

Figs 6A to C: Binding mode and chemical interaction of ligand compound TDU with PRMT2, (A) Solid surface structure of PRMT2, where ligand was colored as green, binding on active site; (B) Three-dimensional representation of TDU with interacted residues on active site; (C) Two-dimensional representation of binding interaction diagram of TDU with PRMT2

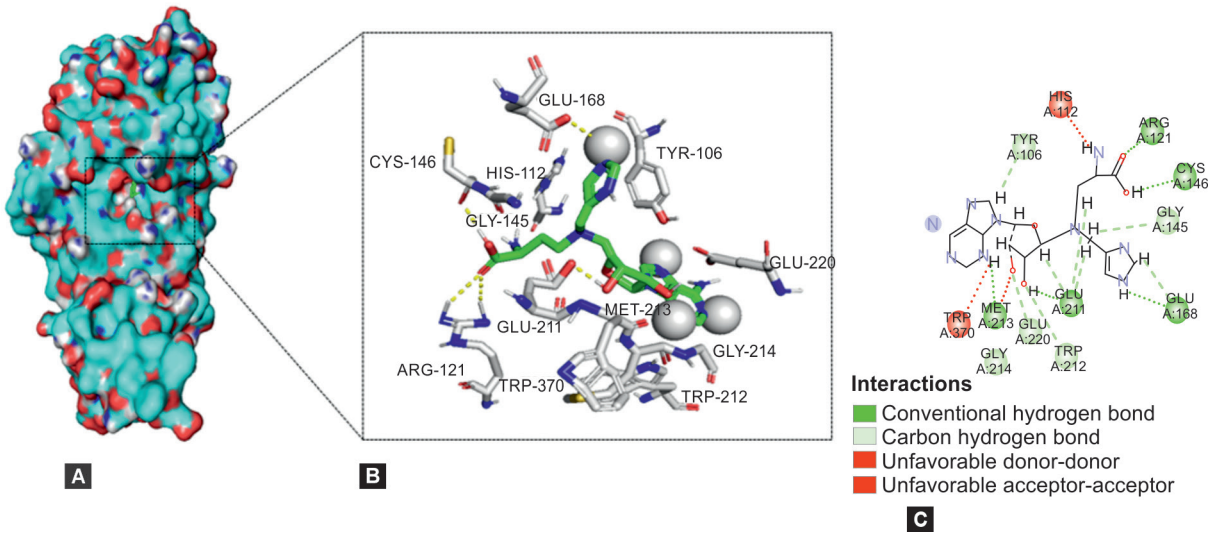

Figs 7A to C: Binding mode and chemical interaction of ligand compound 6DX with PRMT2, (A) Solid surface structure of PRMT2, where ligand was colored as green, binding on active site; (B) Three-dimensional representation of 6DX with interacted residues on active site; (C) Two-dimensional representation of binding interaction diagram of 6DX with PRMT2

residence time. The value of RMSF can be determined by the following equation:

$$\mathrm{RMSF_i} = \sqrt{\frac{1}{N}\sum_{i=1}^{N} \left(r_i'(t) - r_i(t_{ref})\right)^2} \quad \cdots\cdots\cdots\cdots 2$$

Where, T signifies the trajectory time in general; t_{ref} represents the reference or provided time; *r* refers the position of the selected atom in framework I after transposition onto the reference frame. The RMSF curves in Figure 9 show that all three complexes fluctuate at the beginning and at the end.

Most of the fluctuations are observed in the N-terminal and C-terminal of the protein. The fluctuation patterns of the PRMT2-CID: 12422271 and PRMT2-CID: 53346504 complexes are nearly identical, while the fluctuation of the PRMT2-CID: 77620540 complex is slightly higher. PRMT2-CID: 533465904 and PRMT2-CID: 77620540 exhibit fluctuations greater than 3 Å at the beginning and between 300 and 400 residue indexes.

Radius of Gyration Analysis

During a 100 ns simulation, all three complexes have an average Rg of within 3–5 Å, indicating the overall structure's compactness while rotating over an axis (Fig. 10).

These RMSD and RMSF values, as well as Rg ranges for each complex, bolstered the joining of screened potential compounds into PRMT2's active location.

Analysis of SASA and MolSA

The region of a protein that interrelate with its solvent molecules is termed as its SASA. Because the area of every protein residue exposed to the solvent acts as the active site, calculating this area is critical for structural, hydrophobic/hydrophilic, and protein–ligand interaction components. The SASA value of CID: 124222721

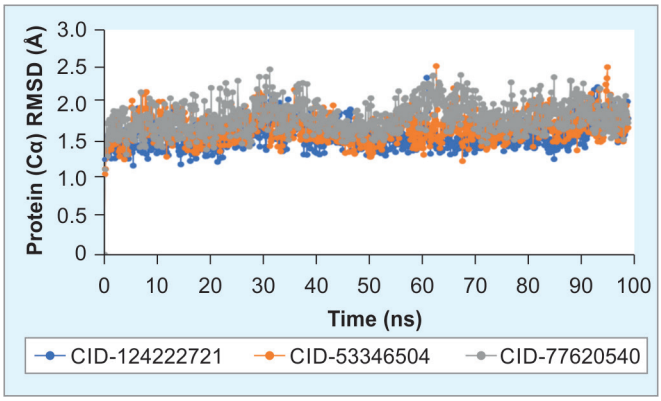

Fig. 8: The RMSD value of the c-alpha atom of three protein–ligand complex for 100 ns

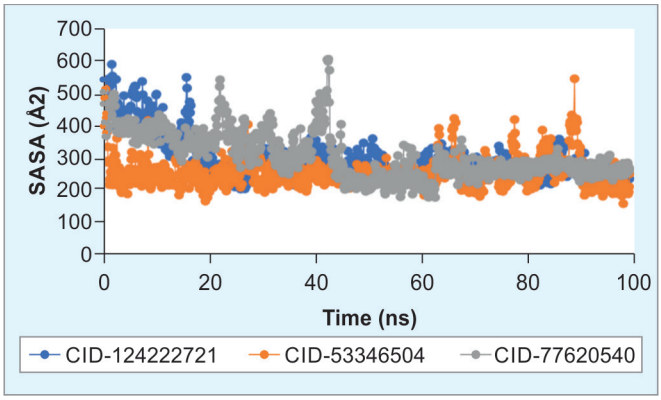

Fig. 11: Protein surface region measured from SASA descriptors of three protein–ligand complexes for 100 ns

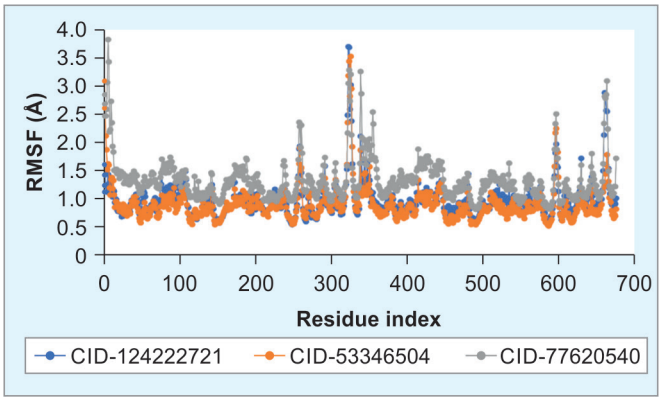

Fig. 9: The RMSF result of three protein–ligand complexes across amino acid residues

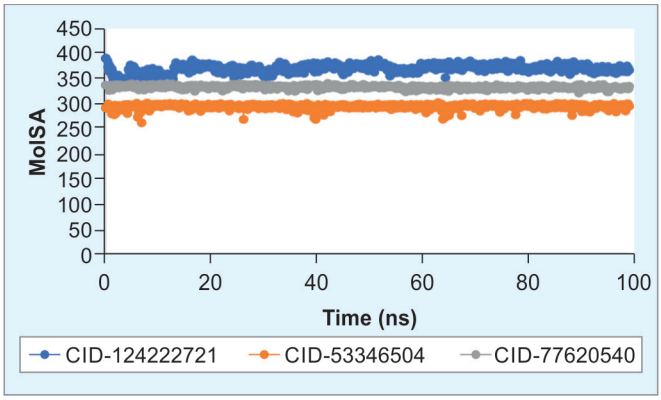

Fig. 12: Molecular surface area (MolSA) of three protein–ligand complex for 100 ns

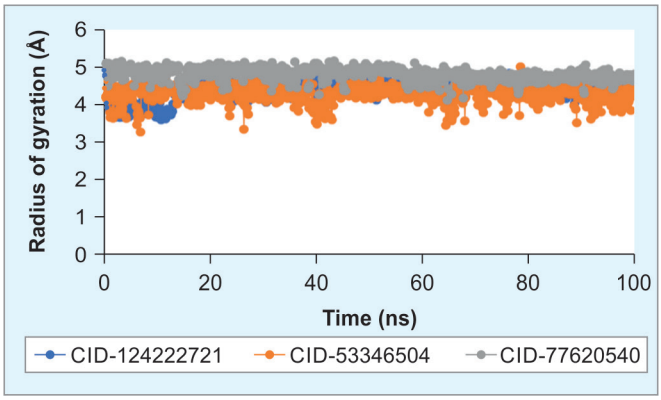

Fig. 10: The radius of gyration profile of three protein–ligand complexes for 100 ns

remined high and exposed a high amount of solvent for 20 ns, then it maintained an average of 300 Å^2 for the rest of the 100 ns time frame. Similarly, compound CID: 77620540 exhibits a high SASA value for approximately 45 ns, after which it remained consistent. The compound CID: 53346504 has an average 250 Å^2 SASA value, indicating the protein–ligand complex did not increment in volume during the process of simulation (Fig. 11).

The molecular surface area (MolSA) is a proximal approximation of the van der Waals surface area where water handled as a solvent is typically depicted by a sphere with a radius of 1.4. Understanding the protein surface and interior cavities with small molecules is critical in structure-based drug design. All the compounds have a standard molecular surface area in this study (Fig. 12).

Analysis of Intramolecular Bonds

The simulation interaction diagram (SID) was utilized to consider the interactions fraction, particular ligand contracts with amino acid residues for a 100 ns simulation time. The ways through which the protein interacted with the ligand molecules were hydrogen bonds, non-covalent bond (hydrophobic bond), ionic interactions, and water bridges. The hydrogen bonding between a ligand and a biological receptor is crucial for the bonding specificity, drug transport, and pharmacokinetics of the ligand.[49,50]

In Figure 13, the stacked bar chart A, which represents compound CID: 124222721, indicates that PRMT2 residues such as GLU^{302}, PRO^{303}, LYS^{332}, and PHE^{364} bind in substantial amounts. For example, PRO^{303} and LYS^{332} have all four types of binding properties: hydrogen, hydrophobic, ionic, and water bridges.

The interaction fraction of the compound CID: 53346504 in the stacked bar chart B shows that protein residues A: GLU^{270}, B: GLU^{119}, B: THR^{123}, and B: PRO^{363} have a greater number of hydrogen bonds.

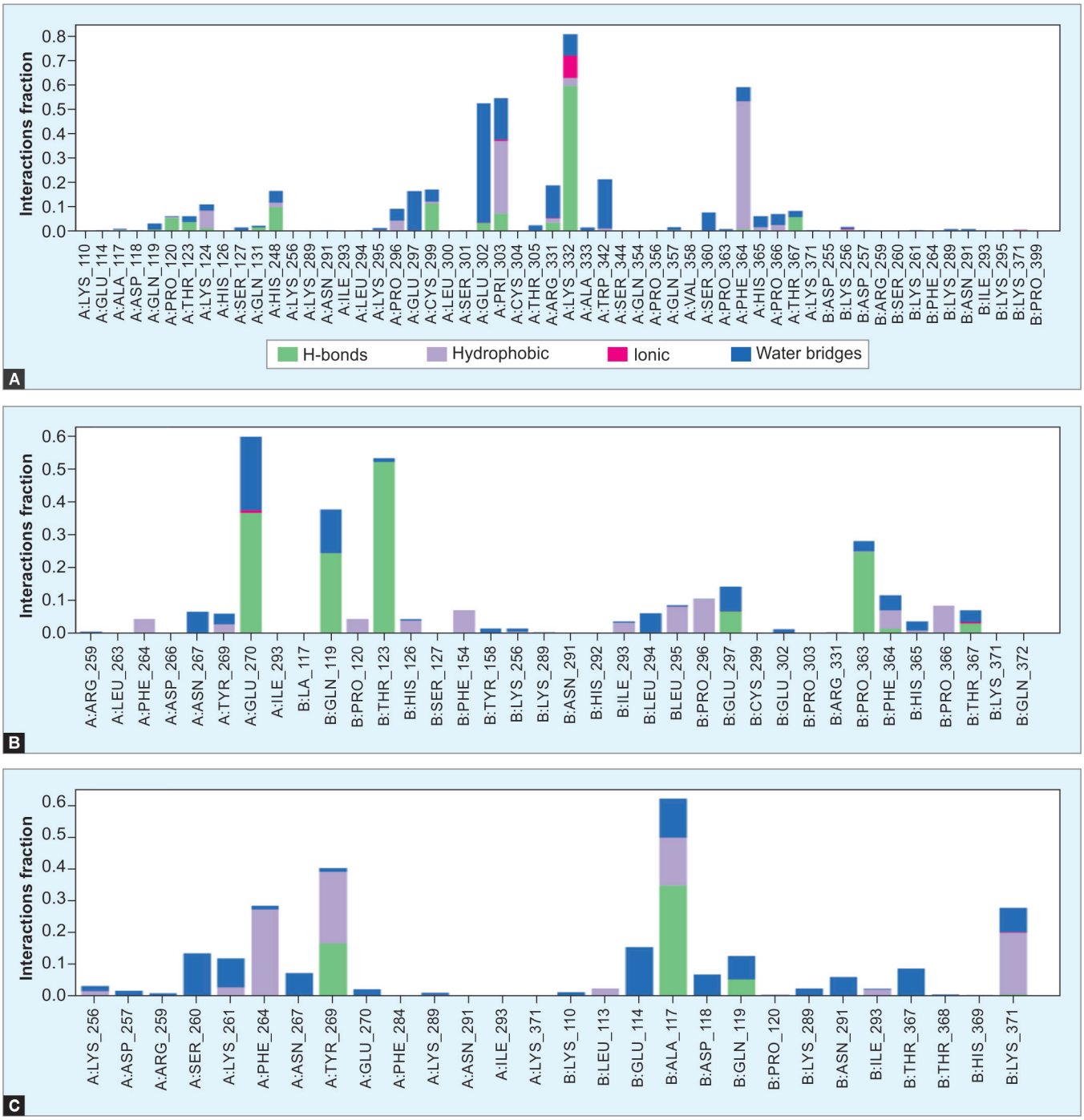

Figs 13A to C: The stacked bar chart depicts the interactions fraction among amino acid residues with ligands compounds of the modeled protein

In the graph, compound CID: 77620540 interacted with PRMT2 active site residues, including A: SER260, A: LYS261, B: GLU114, B: ALA117, and B: LYS371.

Conclusions

The study demonstrated *in silico* molecular characterization of alternatively modeled PRMT2 and predicted three potent inhibitors from 45 inhibitor compounds. We hypothesized that small compounds (inhibitors) from other PRMTs may be related to modifications within the enzyme's movement of PRMT2, and for this reason, recognizable proof of particular inhibitors of PRMT2 is profoundly alluring. Homology modeling methods assessed the three-dimensional structure of the displayed PRMT2. Computational molecular docking studies also demonstrated that our identified three inhibitors, 3BQ, 6DX, and TDU, had higher binding potential. Moreover, the selected three potent inhibitor compounds were non-carcinogenic and possessed acceptable

drug-likeness and toxicological properties. The MD simulations study for the 100 ns time frame, complexes confirmed structural stability and compactness by executing favorable results in RMSD, RMSF, Rg, SASA, MolSA, and intermolecular hydrogen bonding. Further validation as well as experimental inquire, both *in vitro* and *in vivo* testing and applications are required to affirm their adequacy against PRMT2. Further studies will be required to get its role in different cancers including liver cancer and other gastrointestinal cancers.

Data Availability

The data provided in this investigation are available in the article. In addition, the reader may request access to the data used to support the research's findings from the corresponding author.

Authors' Contributions

Conceptualization, MS Hossen, MN Islam, MEA Pramanik;
Formal analysis, MS Hossen, MN Islam, MEA Pramanik, MA Hossain, MMZ Miah, MH Rahman, MS Islam, MA Amin;
Funding acquisition, MEA Pramanik, MMZ Miah FF, Mamun Al Mahtab, Sheikh MF Akbar, MS Islam; Investigation, MEA Pramanik, MMZ Miah FF, AK Sonnyashi, Mamun Al Mahtab, Sheikh MF Akbar;
Methodology, MS Hossen, MN Islam, MEA Pramanik, MA Hossain, MMZ Miah, MH Rahman, MA Amin, ST Antora, FS Sraboni, RN Chowdhury, Nazia Farha, Amina Akter, Samia Sadaf, Farjana Banna, MR Karim, Nasrin Akter;
Resources, MS Hossen, MN Islam, MEA Pramanik, Mamun Al Mahtab, Sheikh MF Akbar;
Software, MS Hossen, MN Islam, MA Hossain, MH Rahman, MA Amin, ST Antora, FS Sraboni, RN Chowdhury, Nazia Farha, Amina Akter, Samia Sadaf, Farjana Banna, MR Karim, Nasrin Akter; Visualization, MS Hossen, MN Islam, MEA Pramanik, MA Hossain;
Writing – Original draft, MS Hossen, MN Islam, MEA Pramanik;
Writing – Review & editing, MN Islam, MEA Pramanik, Mamun Al Mahtab, Sheikh MF Akbar.
The authors Md Sahadot Hossen, Md Nur Islam, and Md Enayet Ali Pramanik contributed equally.
The published version of the research has been reviewed and endorsed by all authors.

Acknowledgments

The authors would like to express their gratitude to the Department of Biochemistry and Molecular Biology at Shahjalal University of Science and Technology in Sylhet, Bangladesh for providing access to their research laboratory facilities.

Supplementary Materials

All the supplementary materials are available online on the website of https://www.ejohg.com/journalDetails/EJOHG.

References

1. Branscombe TL, Frankel A, Lee JH, et al. PRMT5 (Janus Kinase-binding Protein 1) catalyzes the formation of symmetric dimethylarginine residues in proteins. J Biol Chem 2001;276(35):32971–32976. DOI: 10.1074/jbc.M105412200.
2. Lin WJ, Gary JD, Yang MC, et al. The mammalian immediate-early TIS21 protein and the leukemia-associated BTG1 protein interact with a protein-arginine N-methyltransferase. J Biol Chem 1996;271(25):15034–15044. DOI: 10.1074/jbc.271.25.15034.
3. McBride AE, Silver PA. State of the Arg: Protein methylation at arginine comes of age. Cell 2001;106(1):5–8. DOI: 10.1016/S0092-8674(01)00423-8.
4. Chen SL, Loffler KA, Chen D, et al. The coactivator-associated arginine methyltransferase is necessary for muscle differentiation: CARM1 coactivates myocyte enhancer factor-2. J Biol Chem 2002;277(6)4324–4333. DOI: 10.1074/jbc.M109835200.
5. Li H, Park S, Kilburn B, et al. Lipopolysaccharide-induced methylation of HuR, an mRNA-stabilizing protein, by CARM1. J Biol Chem 2002;277(47):44623–44630. DOI: 10.1074/jbc.M206187200.
6. Meister G, Fischer U. Assisted RNP assembly: SMN and PRMT5 complexes cooperate in the formation of spliceosomal UsnRNPs. EMBO J 2002;21(21):5853–5863. DOI: 10.1093/emboj/cdf585.
7. Lukong KE, Richard S. Arginine methylation signals mRNA export RNA editing of a human potassium channel modifies its inactivation. Nat Struct Mol Biol 2004;11(10):914–915. DOI: 10.1038/nsmb1004-914.
8. Bedford MT, Richard S. Arginine methylation: An emerging regulator of protein function. Mol Cell 2005;18(3):263–272. DOI: 10.1016/j.molcel.2005.04.003.
9. Torres-Padilla M-E, Parfitt D-E, Kouzarides T, et al. Histone arginine methylation regulates pluripotency in the early mouse embryo. Nature 2007;445(7124):214–218. DOI: 10.1038/nature05458.
10. Bedford MT, Clarke SG. Protein arginine methylation in mammals: Who, what, and why. Mol Cell 2009;33(1):1–13. DOI: 10.1016/j.molcel.2008.12.013.
11. Pahlich S, Zakaryan RP, Gehring H. Protein arginine methylation: Cellular functions and methods of analysis. Biochim Biophys Acta 2006;1764(12):1890–1903. DOI: 10.1016/j.bbapap.2006.08.008.
12. Feng Y, Maity R, Whitelegge JP, et al. Mammalian protein arginine methyltransferase 7 (PRMT7) specifically targets RXR sites in lysine- and arginine-rich region. J Biol Chem 2013;288(52):37010–37025. DOI: 10.1074/jbc.M113.525345.
13. Yang Y, Hadjikyriacou A, Xia Z, et al. PRMT9 is a Type II methyltransferase that methylates the splicing factor SAP145. Nat Commun 2015;6(1):6428. DOI: 10.1038/ncomms7428.
14. Yang Y, Bedford MT. Protein arginine methyltransferases and cancer. Nat Rev Cancer 2013;13(1)37–50. DOI: 10.1038/nrc3409.
15. Qi C, Chang J, Zhu Y, et al. Identification of protein arginine methyltransferase 2 as a coactivator for estrogen receptor α. J Biol Chem 2002;277(32):28624–28630. DOI: 10.1074/jbc.M201053200.
16. Meyer R, Wolf SS, Obendorf M. PRMT2, a member of the protein arginine methyltransferase family, is a coactivator of the androgen receptor. J Steroid Biochem Mol Biol 2007;107(1–2):1–14. DOI: 10.1016/j.jsbmb.2007.05.006.
17. Oh TG, Bailey P, Dray E, et al. PRMT2 and RORγ expression are associated with breast cancer survival outcomes. Mol Endocrinol 2014;28(7):1166–1185. DOI: 10.1210/me.2013-1403.
18. Yoshimoto T, Boehm M, Olive M, et al. The arginine methyltransferase PRMT2 binds RB and regulates E2F function. Exp Cell Res 2006;312(11):2040–2053. DOI: 10.1016/j.yexcr.2006.03.001.
19. Zhong J, Cao R-X, Zu X-Y, et al. Identification and characterization of novel spliced variants of PRMT2 in breast carcinoma. FEBS J 2012;279(2):316–335. DOI: 10.1111/j.1742-4658.2011.08426.x.
20. Zhong J, Cao R-X, Liu J-H, et al. Nuclear loss of protein arginine N-methyltransferase 2 in breast carcinoma is associated with tumor grade and overexpression of cyclin D1 protein. Oncogene 2014;33(48):5546–5558. DOI: 10.1038/onc.2013.500.
21. Iwasaki H, Kovacic JC, Olive M, et al. Disruption of protein arginine N-methyltransferase 2 regulates leptin signaling and produces leanness in vivo through loss of STAT3 methylation. Circ Res 2010;107(8):992–1001. DOI: 10.1161/CIRCRESAHA.110.225326.
22. Kzhyshkowska J, Kremmer E, Hofmann M, et al. Protein arginine methylation during lytic adenovirus infection. Biochem J 2004;383(2):259–265. DOI: 10.1042/BJ20040210.

23. Scott HS, Antonarakis SE, Lalioti MD, et al. Identification and characterization of two putative human arginine methyltransferases (HRMT1L1 and HRMT1L2). Genomics 1998;48(3):330–340. DOI: 10.1006/geno.1997.5190.
24. Lakowski TM, Frankel A. Kinetic analysis of human protein arginine N-methyltransferase 2: Formation of monomethyl- and asymmetric dimethyl-arginine residues on histone H4. Biochem J 2009;421(2):253–261. DOI: 10.1042/BJ20090268.
25. Cura V, Marechal N, Troffer-Charlier N, et al. Structural studies of protein arginine methyltransferase 2 reveal its interactions with potential substrates and inhibitors. FEBS J 2017;284(1):77–96. DOI: 10.1111/febs.13953.
26. UniPort Consortium. UniProt: The universal protein knowledgebase in 2021. Nucleic Acids Res 2021;49(D1):D480–D489. DOI: 10.1093/nar/gkaa1100.
27. Jones DT. Protein secondary structure prediction based on position-specific scoring matrices. J Mol Biol 1999;292(2):195–202. DOI: 10.1006/jmbi.1999.3091.
28. Geourjon C, Deléage G. SOPMA: Significant improvements in protein secondary structure prediction by consensus prediction from multiple alignments. Comput Appl Biosci 1995;11(6):681–684. DOI: 10.1093/bioinformatics/11.6.681.
29. Waterhouse A, Bertoni M, Bienert S, et al. SWISS-MODEL: Homology modelling of protein structures and complexes. Nucleic Acids Res 2018;46(W1):W296–W303. DOI: 10.1093/nar/gky427.
30. Krieger E, Joo K, Lee J, et al. Improving physical realism, stereochemistry, and side-chain accuracy in homology modeling: Four approaches that performed well in CASP8. Proteins 2009;77(Suppl 9):114–122. DOI: 10.1002/prot.22570.
31. Kemmish H, Fasnacht M, Yan L. Fully automated antibody structure prediction using BIOVIA tools : Validation study. PLoS One 2017;12(5):e0177923. DOI: 10.1371/journal.pone.0177923.
32. Laskowski RA, MacArthur MW, Moss DS, et al. PROCHECK: A program to check the stereochemical quality of protein structures. 1993;26(2):283–291. DOI: 10.1107/S0021889892009944.
33. Colovos C, Yeates TO. Verification of protein structures: Patterns of nonbonded atomic interactions. Protein Sci 1993;2(9):1511–1519. DOI: 10.1002/pro.5560020916.
34. Ramachandran GN, Ramakrishnan C, Sasisekharan V. Stereochemistry of polypeptide chain configurations. J Mol Biol 1963;7(1):95–99. DOI: 10.1016/S0022-2836(63)80023-6.
35. Lill MA, Danielson ML. Computer-aided drug design platform using PyMOL. J Comput Aided Mol Des 2011;25(1):13–19. DOI: 10.1007/s10822-010-9395-8.
36. Kumar S, George TY, Meng Z, et al. Protein arginine methyltransferases: Insights into the enzyme structure and mechanism at the atomic level. Cell Mol Life Sci 2019;76(15):2917–2932. DOI: 10.1007/s00018-019-03145-x.
37. Smith E, Zhou W, Shindiapina P, et al. Recent advances in targeting protein arginine methyltransferase enzymes in cancer therapy. Expert Opin Ther Targets 2018;22(6):527–545. DOI: 10.1080/14728222.2018.1474203.
38. Feldman HJ, Snyder KA, Ticoll A, et al. A complete small molecule dataset from the protein data bank. FEBS Letters 2006;580(6):1649–1653. DOI: 10.1016/j.febslet.2006.02.003.
39. Kim S, Chen J, Cheng T, et al. PubChem 2019 update: Improved access to chemical data. Nucleic Acids Res 2019;47(D1):D1102–D1109. DOI: 10.1093/nar/gky1033.
40. Hanwell MD, Curtis DE, Lonie DC, et al. Avogadro: An advanced semantic chemical editor, visualization, and analysis platform. J Cheminform 2012;4(1):17. DOI: 10.1186/1758-2946-4-17.
41. Salha D, Andaç M, Denizli A. Molecular docking of metal ion immobilized ligands to proteins in affinity chromatography. J Mol Recognit 2021;34(2):e2875. DOI: 10.1002/jmr.2875.
42. Tian W, Chen C, Lei X, et al. CASTp 3.0: Computed atlas of surface topography of proteins. Nucleic Acids Res 2018;46(W1):W363–W367. DOI: 10.1093/nar/gky473.
43. Harder, E, Damm W, Maple J, et al. OPLS3: A force field providing broad coverage of drug-like small molecules and proteins. J Chem Theory Comput 2016;12(1):281–296. DOI: 10.1021/acs.jctc.5b00864.
44. Hasan A, Mazumder HH, Chowdhury AS, et al. Molecular-docking study of malaria drug target enzyme transketolase in Plasmodium falciparum 3D7 portends the novel approach to its treatment. Source Code Biol Med 2015;10(1):7. DOI: 10.1186/s13029-015-0037-3.
45. Hughes JP, Rees S, Kalindjian SB, et al. Principles of early drug discovery. Br J Pharmacol 2011;162(6):1239–1249. DOI: 10.1111/j.1476-5381.2010.01127.x.
46. Raj S, Sasidharan S, Dubey VK, et al. Identification of lead molecules against potential drug target protein MAPK4 from L. Donovani: An in-silico approach using docking, molecular dynamics and binding free energy calculation. PLoS One 2019;14(8):1–20. DOI: 10.1371/journal.pone.0221331.
47. Zhu K, Jiang C-S, Hu J, et al. Interaction assessments of the first S-adenosylmethionine competitive inhibitor and the essential interacting partner methylosome protein 50 with protein arginine methyltransferase 5 by combined computational methods. Biochem Biophys Res Commun 2018;495(1):721–727. DOI: 10.1016/j.bbrc.2017.11.089.
48. Sun, Y, Wang Z, Yang H, et al. The development of tetrazole derivatives as protein arginine methyltransferase I (PRMT I) inhibitors. Int J Mol Sci 2019;20(15):3840. DOI: 10.3390/ijms20153840.
49. Gancia E, Montana JG, Manallack DT. Theoretical hydrogen bonding parameters for drug design. J Mol Graph Model 2001;19(3–4):349–362. DOI: 10.1016/S1093-3263 (00)00084-X.
50. Varma AK, Patil R, Das S, et al. Optimized hydrophobic interactions and hydrogen bonding at the target-ligand interface leads the pathways of drug-designing. PLoS One 2010;5(8):e12029. DOI: 10.1371/journal.pone.0012029.